Chemical Physics 56 (1981) 327–335
North-Holland Publishing Company

# A THEORETICAL STUDY OF THE REACTION OF Mg(3s3p $^3$P) WITH $H_2$

Noah ADAMS, W.H. BRECKENRIDGE and Jack SIMONS [‡]
*Department of Chemistry, University of Utah, Salt Lake City, Utah 84112, USA*

Received 14 October 1980

Theoretical calculations on relevant portions of the potential surface of the first triplet state of $MgH_2$ were carried out at the SCF and MCSCF CI level in order to learn more about the detailed mechanism of the reaction Mg(3s3p $^3$P) + $H_2 \rightarrow$ MgH + H. It was found that this reaction can proceed with essentially no activation barrier (≤1.8 kcal/mole) above the reaction's 11–12 kcal/mole endothermicity via side-on attack by Mg($^3$P) of the H–H bond, whereas end-on attack gives rise to a barrier of ≈14 kcal/mole above the endothermicity. Analysis of the orbital occupancy variations along the $C_{2v}$ side-on approach coordinate indicates that $Mg^+–H_2^-$ partial charge-transfer interactions are important. No indication of a bound or metastable triplet state of $MgH_2$ was found.

## 1. Introduction

Since the discovery in 1922 that hydrogen atoms were produced when a mercury/hydrogen gas mixture was irradiated with a mercury resonance lamp (i.e., the first demonstration of photosensitization) [1], there has been sustained interest in the rates and mechanisms by which electronically excited metal atoms are deactivated by $H_2$, the simplest molecular quencher [1–7]. Callear and McGurk [5] have shown unequivocally that the rapid quenching of excited Hg(6s6p $^3P_1$) and Hg(6s6p $^3P_0$) by $H_2$ is, in fact, entirely chemical in nature, with production of HgH + H approximately twice as likely as that of Hg(6s$^2$ $^1S_0$) + H + H. Experiments with the analogous group IIb excited states, Cd(5s5p $^3P_J$) and Zn(4s4p $^3P_J$), (for which there is insufficient energy for direct scission of the H–H bond) have also demonstrated near-gas-kinetic quenching rates by $H_2$, with production of CdH and ZnH as dominant exit channels [4,6,7].

On the other hand, the quenching of excited Mg(3s3p $^3P_J$) by $H_2$ at moderate temperatures has been found to be four orders of magnitude slower than the gas kinetic limit [8,9]. A recent accurate determination of the bond strength of MgH [11] allows a quite reasonable explanation for the inefficient quenching within the context of chemical exit-channel control for all of these excited triplet state processes [4]. Reaction (1) below is thus presumed to be slow because it is endothermic by 11.5 ± 0.5 kcal/mole:

$$Mg(^3P_J) + H_2 \rightarrow MgH + H. \tag{1}$$

Recent experiments have shown that the rate of quenching of Mg($^3P_J$) by $H_2$ is indeed strongly temperature dependent [9]. The data have been rationalized nicely by assuming that at low temperatures very inefficient electronic-to-vibrational (E-to-V) energy transfer dominates, while at high temperatures reaction (1) is rate-controlling and has no activation energy beyond the 11.5 kcal/mole endothermicity.

In marked contrast to the predominantly chemical interactions of the Hg, Cd, Zn and Mg excited states with $H_2$, the excited states of the alkali metals are quenched with high efficiency at low temperatures despite the fact that analogous production of the alkali metal hydrides is quite endothermic in every case [11–14]. This efficient E-to-V quenching by $H_2$ of the excited alkali metals has been explained by means of models [15] in which potential surfaces of $M^+H_2^-$ character (where M is an alkali metal) are sufficiently low in energy, because of the low ionization potentials of M, to facilitate crossings between entrance M($^2$P)–$H_2$ and exit M($^2$S)–$H_2(v)$ surfaces.

---

[‡] Camille and Henry Dreyfus Fellow, John Simon Guggenheim Fellow.

These rather crude electrostatic models are still controversial [15], but have been given some measure of respectability by a recent close-coupling theoretical calculation [16] in which the quenching of Na(3p $^2$P) by $H_2$ was shown to occur from a single excited-state surface of predominantly charge transfer character. It has been postulated [4,9] that the slow E-to-V transfer rate in the Mg($^3$P)–$H_2$ case is due to the fact that analogous surfaces of $Mg^+H_2^-$ character are too high in energy because of the greater ionization potential of magnesium.

In an attempt to understand in greater detail the mechanism of quenching of excited metal atoms by $H_2$, we have performed ab initio theoretical calculations on the especially relevant portions of the lowest energy triplet potential surface on which reaction (1) occurs. Because of the broad interest in such E-to-V and chemical quenching processes, as discussed above, and because Mg + $H_2$ involves few enough electrons to facilitate accurate theoretical calculations, the first triplet-state potential surface of $MgH_2$ appeared to us to offer an ideal prototype for a theoretical study of excited metal atom quenching processes.

Our theoretical treatment of the mechanism of reaction (1) has centered on several themes. First, in light of the absence of activation barriers for the reactions of the analogous triplet states of the group IIb metals with $H_2$, and the postulate that reaction (1) occurs with no substantial activation energy beyond the endothermicity, it is certainly important to determine if there is indeed a reaction pathway on the triplet $MgH_2$ potential surface for which the activation barrier is approximately 11.5 kcal/mole (the endothermicity). Also of interest in this regard is the possibility of preferential orientation in the attack of $H_2$ by Mg($^3$P), i.e., side-on (insertion) or end-on (abstraction). Second, because of the possibility of charge transfer in these systems, it is important to examine the Mg($^3$P)–$H_2$ wavefunction for any indication of the onset of charge-transfer-like character. Finally, the possibility of a bound triplet state or a metastable geometric configuration of triplet $MgH_2$ needs to be explored. Calculations of the potential surface for reaction (1) were carried out at the spin- and spatially-unrestricted self-consistent field (SCF) level, and, to a limited extent, at the multi-configurational SCF level. It was not our intention to obtain a highly accurate description of the full three-dimensional triplet potential energy surface. Rather, we wanted to explore particularly interesting regions of the surface to search for the above mentioned chemically relevant aspects of the interaction potential.

## 2. Atomic orbital basis set

The unrestricted SCF calculations pertaining to the Mg($^3$P) + $H_2$ potential energy surface were performed

Table 1
Large basis set

| | | $\alpha$ | $C$ |
|---|---|---|---|
| Mg | $\phi_{1s}$ | 29196.31 | 0.0068144 |
| | | 5189.496 | 0.0412912 |
| | | 1307.748 | 0.1982789 [a] |
| | | 372.6497 | 0.8212065 |
| | $\phi_{2s}$ | 119.1241 | 0.2213597 |
| | | 43.52120 | 0.4086057 |
| | | 17.52420 | 0.3772874 |
| | | 7.167605 | 0.0983273 |
| | $\phi_{3s}$ | 24.33906 | 1 |
| | $\phi_{4s}$ | 2.381539 | 1 |
| | $\phi_{5s}$ | 0.816411 | 1 |
| | $\phi_{6s}$ | 0.129611 | 1 |
| | $\phi_{7s}$ | 0.0634204 | 1 |
| | $\phi_{8s}$ | 0.0278351 | 1 |
| | $\phi_{1p}$ | 192.644 | 0.00475 |
| | | 45.7493 | 0.03462 |
| | | 14.2558 | 0.14372 |
| | | 4.9324 | 0.34665 |
| | $\phi_{2p}$ | 1.78234 | 0.46489 |
| | | 0.6151 | 0.24109 |
| | $\phi_{3p}$ | 0.15125 | 1 |
| | $\phi_{4p}$ | 0.0451 | 1 |
| H | $\phi_{1s}$ | 13.3615 | 0.130844 |
| | | 2.0133 | 0.921539 |
| | $\phi_{2s}$ | 0.4538 | 1 |
| | $\phi_{3s}$ | 0.12330 | 1 |
| | $\phi_{4s}$ | 0.03 | 1 |
| | $\phi_{1p}$ | 0.29891 | 1 |

---

[a] Correction of misprint in Huzinaga's paper. Was reported as 0.0982789.

using the MOLECULE integral package and the GREENFNC SCF program. The reasonably large contracted gaussian basis (8s4p Mg; 4s1p H), listed in table 1, which was used to explore the most significant region of the potential surface, was constructed in the following manner.

The Mg atomic orbital (AO) basis is a modified version of the double-zeta contracted gaussian (CGTO) bases of Huzinaga [17] and Veillard [18]. The s-type functions were taken from Huzinaga whereas the p-type functions were obtained from Veillard. The two "tight" s-type contracted functions of Huzinaga were left intact and are labeled $\phi_{1s}$ and $\phi_{2s}$ in table 1. Huzinaga's two remaining contracted s-type functions were then uncontracted to give more flexibility to the basis. The tightest two primitive functions thus obtained were left unaltered. Since each of these latter two contracted functions contained a primitive gaussian with an exponent of $\approx 0.8$ (0.80 versus 0.83), only one such primitive function (whose gaussian exponent is the geometric mean of the above) was employed. The two most diffuse primitives of Huzinaga were replaced by three new functions. One of these three ($\phi_7$) has an exponent equal to the geometric mean of the two Huzinaga functions. The two remaining functions, $\phi_{6s}$ and $\phi_{8s}$ were obtained by varying the orbital exponents of these functions to minimize the Mg($^1$S) energy. The two p-type contracted gaussian functions from Veillard's basis were left intact and are labeled in table 1 as $\phi_{1p}$ and $\phi_{2p}$. To these functions were added two diffuse primitive p-type functions whose orbital exponents were then varied to minimize the Mg($^3$P) energy at the SCF level.

The hydrogen AO basis was obtained by adding a diffuse s-type and a p-type function to the (4s/3s) CGTO set of Dunning [19]. The exponents of these additional functions were varied to minimize the SCF energy of MgH($^2\Sigma^+$) at its experimental equilibrium bond length of 3.27 au. After this orbital optimization, variation of the MgH bond length gave rise to an optimal MgH bond length of 3.28 au, which compares well with the experimental value. The optimized exponents of the additional s- and p-type hydrogen atom basis functions are rather small because the bonding in MgH is quite polar, with the more electronegative hydrogen being negative.

The purpose of constructing the above orbital basis set was to obtain a basis which is flexible enough to give a reliable description of the potential surface at all geometries, and yet small enough to allow a reasonable calculation time. The basis sets of neither Huzinaga nor Veillard were designed for description of excited atomic states. Furthermore, treatments of $MgH_2$($^1\Sigma$) by Ahlrichs et al. [20] and of MgH($^2\Sigma^+$) by Meyer and Rosmus [21] indicate the necessity of including polarization functions (p orbitals) on hydrogen. Ahlrichs reported that inclusion of polarization functions on Mg seemed to be unimportant even at the configuration interaction (CI) level, and attributed this to the ionic nature of the magnesium

Table 2
Comparison of calculated energies in the present work to values obtained by other investigators at the SCF level

| System | This work | Other workers | Reference | Basis size |
|---|---|---|---|---|
| Mg($^1$S) | −199.605823 au | −199.607500 au<br>−199.59312 au | Huzinaga [17]<br>Veillard [18] | (14s7p/4s2p) CGTO<br>(12s6p/6s2p) CGTO |
| Mg($^1$S) → Mg($^3$P) | 42.89 kcal/mole | 42.3219 kcal/mole<br>41.3319 kcal/mole | Liu [22] | (8s6p3d1f) STO [a] |
| $MgH_2$($^1\Sigma$) → Mg($^1$S) + 2 H | 76.94 kcal/mole | 77.77 kcal/mole | Ahlrichs [20] | Mg(11s7p1d/7s4p1d) CGTO<br>H(5s1p/351p) CGTO |
| MgH → Mg($^1$S) + H | 25.87 kcal/mole | 26.5 kcal/mole<br>26.65 kcal/mole | Meyer [21]<br>Liu [22] | Mg(13s8p3d1f)<br>H(7S2p2d)<br>(contraction information not given) |

[a] The two values reported were attributed to the imposition of $C_{\infty v}$ symmetry in the calculation of "Mg($^3\Pi$)" and "Mg($^3\Sigma$)", respectively.

hydrides. In light of these facts and the greater calculational cost of adding d-type functions to the Mg AO basis, no attempt was made to do so.

The reliability of the resulting basis may be tested by comparing SCF-level properties obtained with it to those of other workers. This comparison is summarized in table 2, from which it is seen that the absolute energies and energy differences obtained in this work compare quite well (within 1 kcal/mole) with those given by other workers using much larger basis sets. We therefore have reason to believe that our basis is capable of giving good SCF-level descriptions of Mg($^3$P), MgH and $MgH_2$.

In addition to the large basis described above, a smaller (approximately minimal) basis was used for exploratory work aimed at examining the qualitative features of the triplet $MgH_2$ potential energy surface. This basis consists of a much contracted version of the Mg basis (added p-type functions included) and Dunning's (4s/2s) CGTO basis for hydrogen (no added functions). It was found that the results obtained from this minimal basis were in qualitative agreement (i.e., geometrically accurate with regard to surface features) with those of the large basis in cases where one hydrogen was farther away from magnesium than the other. The small basis was, however, unreliable for predictions of the behavior of near-$C_{2v}$ geometries, which is consistent with the earlier mentioned observation concerning the importance of partial charge transfer in $MgH_2$ which would require diffuse orbitals and polarization functions on hydrogen.

## 3. Construction of the MCSCF and CI wavefunctions

MCSCF CI calculations employing a large gaussian basis were performed using the Utah MCSCF and CI programs (both employing the unitary group approach) which were developed by Dr. R. Shepard. These more extensive calculations were limited to a small region of the $C_{2v}$ part of the potential surface where a saddle point and a local minimum were encountered in the SCF-level study described in section 4. The procedure used to obtain the MCSCF-CI energies at these critical points on the potential energy surface can be outlined as follows.

An 88-configuration MCSCF calculation was performed at each geometrical point of interest in order to obtain optimized orbitals for use in the subsequent CI calculations. This oribtal optimization was done to reduce the number of configurations needed to achieve a good CI-level description of the wavefunction, compared to that which would have been required if the SCF orbitals had been used. The distinct row table (DRT) used within our unitary group program to describe the MCSCF configuration generated all single and double and certain (few) triple excitations among the valence oribtals of $MgH_2$. Excitation out of the $4a_1(H_2\sigma_g)$, $5a_1$(Mg 3s) and $2b_2$(Mg 3p) orbitals into the lowest two virtual orbitals of each symmetry (except for $a_2$ symmetry which contains only one $2p\pi_g$ function on $H_2$) were found to be adequate to give a reasonably accurate yet compact CI wavefunction. No excitations out of the core orbitals (Mg 1s, 2s, 2p) were included. At the potential surface's saddle point (as determined by the SCF-level study outlined below), a full CI calculation within the MCSCF excitation subspace (250 configurations) gave an energy only 0.20 kcal/mole lower than the all single and double (and few triple) excitations MCSCF energy mentioned above, indicating that contributions from most triple and quadruple excitations are insignificant.

Since the saddle point (which is usually associated with an avoided crossing of two electronic states) and the nearby local minimum were expected to have wavefunctions of different configurational character, it was necessary to include in our final MCSCF-CI calculations all configurations which were found to be important at either geometry in order to give a reliable description of these two points and the neighboring regions of the surface. Therefore, configuration selection CI calculations were performed at the saddle point and the local minimum in order to determine the list of configurations needed to give a good description at either geometry. These selection oriented CI wavefunctions included the MCSCF configuration lists which were used previously at the saddle and local minimum together with all single excitations (excluding core excitations) from the dominant configuration in the MCSCF function into all virtual orbitals which were not occupied in the MCSCF wavefunctions. By using the squares of the CI expansion coefficients as an estimate of the importance of individual configurations, all singly excited configurations which were estimated to contribute at least $10^{-5}$ hartree to the energy of either the saddle point or the local minimum were labeled for inclusion in the CI excitation space. The virtual orbitals arising in these important singly excited configurations were labeled as important virtuals. Our final CI configuration space was then formed by taking the original MCSCF configuration space plus all single and double excitations from the ground configuration into the above described important virtual orbitals, thereby giving a total of 850 configurations. As before, no excitations from core orbitals were allowed.

At the saddle point, the valence correlation energy obtained from this larger calculation was found to be 33.9 kcal/mole (relative to a single configuration MCSCF wavefunction). Since the corresponding value for the 88-configuration MCSCF calculation was only 5.65 kcal/mole less (16.7%), it is felt that most of the valence correlation energy was obtained from the MCSCF CI procedure outlined above.

## 4. Results and discussion

The valence atomic orbitals of Mg(3s, 3p) and $H_2(1\sigma_g, 1\sigma_u)$ belong to $C_{2v}$ symmetries $a_1$, $b_1$ and $b_2$. The lowest energy triplet configuration of $Mg(^3P) + H_2$ is expected to be dominated by the orbital occupancy $4a_1^2(1\sigma_g^2)5a_1(3s\ Mg)2b_2(3p\ Mg)$. Of course the $2b_2$ orbital could be replaced by either of the other 3p Mg orbitals $6a_1$ or $2b_1$ because they are degenerate for separated reactants. However, the $6a_1$ and $2b_1$ 3p orbitals of Mg are not expected to result in attractive interactions with the $H_2$ molecule for this $C_{2v}$ approach geometry. The $2b_1$ orbital is essentially non-bonding and the $6a_1$ 3p orbital results in repulsive interaction with the $\sigma_g^2$ $H_2$ molecule. These same valence atomic orbitals combine to form the bonding ($4a_1$ and $2b_2$) and antibonding ($a_1$ and $b_2$) orbitals of $C_{2v}$ $MgH_2$ as well as the $sp^2$ lone pair hybrid orbital ($5a_1$) and the non-bonding $3p_\pi$ orbital ($2b_1$) of $MgH_2$. The lowest energy triplet state of $MgH_2$ is expected to be described by the orbital occupancy $4a_1^2$(MgH bond)$2b_2$(MgH bond)$5a_1$(Mg lone pair). Because the dominant orbital occupancies of $Mg(^3P) + H_2$ and $MgH_2(^3B_2)$ are identical, it is expected that a single configuration unrestricted SCF treatment of the $C_{2v}$ part of the reaction potential energy surface should be adequate.

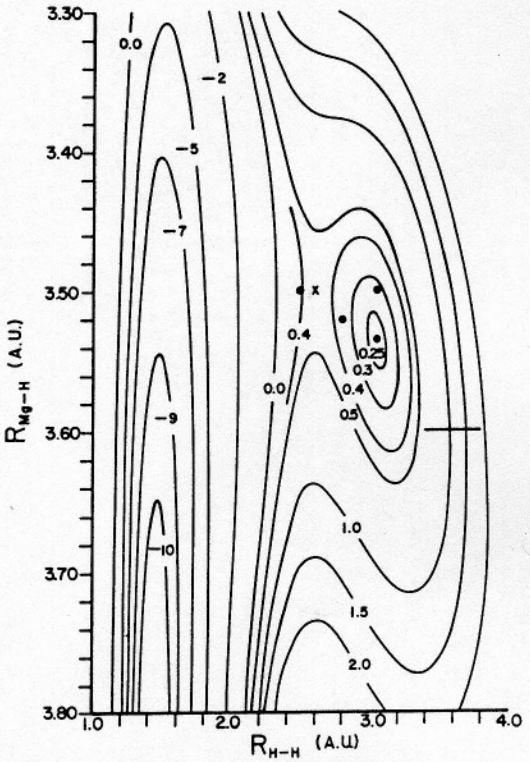

Fig. 1. A contour plot of the potential surface of the first triplet state of $MgH_2$. The energies are in kcal/mole and are relative to the energy of $MgH(^2\Sigma) + H$. See the text for explanation of the dots, cross, and horizontal line.

Since Walsh's rules predict a $C_{2v}$ geometry for a bound triplet state of $MgH_2$, it was necessary to make an extensive characterization of the $C_{2v}$ part of the potential surface within the limits of reasonable internuclear distances. Using the known $H_2$ and MgH equilibrium bond lengths (1.4 au and 3.27 au) as guides, a region of the $C_{2v}$ surface was mapped out at the unrestricted SCF level (for $^3B_2$ $MgH_2$) by varying the Mg-to-H distance from 3.3 to 3.8 au and the H-to-H distance from ≈1.0 to 4.0 au. A contour plot of this part of the potential energy surface, generated from a polynomial least-squares fit to 36 calculated SCF energies, may be found in fig. 1. The following polynomial was found to give a reasonable fit of these SCF energies without introducing extraneous "wiggles":

$$E = \sum_{k=1}^{2} \frac{B_k}{r_k} + \sum_{i=0}^{3} \sum_{j=0}^{5} C_{ij} r_1^i r_2^j, \qquad (2)$$

Table 3
Coefficients of the polynomial [eq. (2)] used to fit the potential energy values obtained here for the first triplet state of $MgH_2$

|  | $k$ | $B_k$ |
|---|---|---|
|  | 1 | −0.78603095D+00 |
|  | 2 | 0.38130821D+02 |
| $i$ | $j$ | $C_{ij}$ |
| 0 | 0 | −0.25891086D+03 |
| 0 | 1 | 0.43582246D+02 |
| 0 | 2 | −0.30516535D+02 |
| 0 | 3 | 0.10623044D+02 |
| 0 | 4 | −0.17459018D+01 |
| 0 | 5 | 0.10625770D+00 |
| 1 | 0 | 0.12386846D+02 |
| 1 | 1 | −0.28976112D+02 |
| 1 | 2 | 0.22237160D+02 |
| 1 | 3 | −0.80097994D+01 |
| 1 | 4 | 0.13398807D+01 |
| 1 | 5 | −0.82413051D−01 |
| 2 | 0 | −0.33460360D+01 |
| 2 | 1 | 0.77553996D+01 |
| 2 | 2 | −0.59723334D+01 |
| 2 | 3 | 0.21569507D+01 |
| 2 | 4 | −0.36186486D+00 |
| 2 | 5 | 0.22339371D−01 |
| 3 | 0 | 0.30208309D+00 |
| 3 | 1 | −0.69953620D+00 |
| 3 | 2 | 0.54199122D+00 |
| 3 | 3 | −0.19646819D+00 |
| 3 | 4 | 0.33071063D−01 |
| 3 | 5 | −0.20502897D−02 |

where $r_1$ is the Mg–H distance and $r_2$ is the H–H distance. The coefficients $B_k$ and $C_{ij}$ are given in table 3.

The topology of the $C_{2v}$ surface is dominated by three main features. The first of these is the entrance channel, which is repulsive with respect to the approach of Mg towards $H_2$. Along the minimum energy path within this channel, the H–H distance corresponds closely to the $H_2$ equilibrium bond length, although it increases slightly as the Mg approaches. There is little left-right curvature in the surface along the minimum-energy path, hence it would not be expected that relative translational energy alone would enhance the production of MgH + H.

Two additional features are encountered as the H–H distance is increased from beyond its equilibrium bond length of ≈1.4 au. For Mg–H distances greater than 3.4 au, the potential energy increases as the hydrogens are separated, until a "ridge", which is roughly characterized by a constant H–H distance of 2.6 au, is encountered. As the H–H distance is increased beyond 2.6 au, a shallow depression (the above mentioned local minimum) is exhibited. For Mg–H distances less than 3.4 au, separation of the hydrogens beyond ≈1.4 au is completely repulsive. Thus, at the SCF level, the $C_{2v}$ potential surface exhibits a shallow well which is separated from the entrance channel by a small potential barrier. The saddle point of the barrier, located at an Mg–H distance of 3.5 au and an H–H distance of 2.6 au, was found to lie 0.35 kcal/mole above MgH + H. The local minimum, located at an Mg–H distance of ≈3.54 au and an H–H distance of ≈3.05 au, was found to lie less than 0.25 kcal/mole above the MgH + H energy. Needless to say, the accuracy of these tentative observations should be questioned. Barriers and local minima of the sizes obtained here may be artifacts of the calculational method. For this reason, we decided to examine these aspects of the surface under higher resolution.

Since the only minimum found on the SCF-level $C_{2v}$ surface is higher in energy than Mg($^3$P) + $H_2$, it can be concluded that no thermodynamically stable triplet state of $MgH_2$ having $C_{2v}$ symmetry exists. However, the existence of the small well at the SCF-level presents the possibility of a metastable state of $MgH_2$ (having a lifetime of one or more vibrations). Due to the frequent unreliability of such SCF-level extrema, MCSCF-CI calculations were performed at the saddle point and local minimum geometries, using the procedure outlined in section 3. At the MCSCF-CI level, the energy at the geometry of the saddle point was found to be 0.47 kcal/mole *below* that of the local minimum. Additional MCSCF-CI calculations at points denoted by dots in fig. 1, which lie between and in the immediate vicinity of the SCF saddle point (denoted by an X) and local minimum, showed that the potential energy increases monotonically along paths connecting the entrance channel and the SCF "well region". There is no saddle point or well at the MCSCF level. However, the general plateau region lying between $2.4 \leqslant R_{HH} \leqslant 3.6$ au and $3.4 \leqslant$

$R_{MgH} \leqslant 3.6$ remains interesting from the point of view of being a likely entry to the MgH + H reaction exit channel.

In addition to the energetics of the $C_{2v}$ surface, the physical nature of the interaction in various parts of this surface is also of interest. This is best demonstrated by the behavior of the valence $4a_1$, $5a_1$, and $2b_2$ orbitals as functions of geometry. Within the entrance channel, the SCF orbital expansion coefficients for these orbitals indicate that the character of the system is predominantly that of $H_2$ and $Mg(^3P)$. The $4a_1$ orbital, doubly occupied throughout the surface, is structured most like an $H_2\,\sigma$ bonding orbital with little contribution from Mg. The $5a_1$ and $2b_2$ orbitals, both singly occupied with $\alpha$ spin, have the character of Mg 3s and 3p ($b_2$) orbitals, respectively, with little contribution from the hydrogens. With increasing H–H distance, the SCF energies of the $5a_1$ and $2b_2$ orbitals cross at a geometry coinciding with the saddle of fig. 1. In the region of this saddle, the singly occupied $2b_2$ orbital shows roughly equal contributions from Mg 3p ($b_2$) and $H_2\,\sigma^*$ orbitals. Upon further separation of the hydrogens (motion into the depression and beyond), the Mg contribution to the $2b_2$ orbital diminishes and the $H_2\,\sigma^*$ component increases. Hence, we do see significant Mg to $H_2$ charge transfer within this $2b_2$ orbital. The $5a_1$ orbital maintains its Mg character, whereas the $4a_1$ orbital begins to involve some mixing of Mg 3p and 3s with the dominant $H_2\,\sigma_g$ orbital. However, we do not see evidence for the formation of full Mg–H bonds one would expect to see for a stable or metastable triplet $MgH_2$. Thus, the system changes in behavior from that of a repulsive interaction between nearly distinct $Mg(^3P)$ and $H_2$ in the entrance channel to that of a state with considerable charge transfer character in the region beyond the saddle point. Although this state possesses considerable charge transfer character, it is still largely covalent.

Since it is necessary that the $C_{2v}$ symmetry be broken in order for the system to go to the products MgH + H, the transition from $C_{2v}$ to asymmetric geometries ($C_s$) was investigated in the region of the SCF-level "well" to determine whether there is a barrier to breaking the symmetry, and to locate the minimum-energy exit point from the $C_{2v}$ surface. Due to the three dimensional nature of the surface, the H–H distance was first frozen. Then, to compare $C_{2v}$ and $C_s$ behavior for a given H–H distance, the Mg was moved along isomeric elliptical ($R_{MgH1} + R_{MgH2}$ = constant) and hyperbolic ($R_{MgH1} - R_{MgH2}$ = constant) paths. The results of these $C_s$ SCF-level calculations indicate that at H–H separations greater than 3.8 au, the path from $C_{2v}$ to asymmetric geometries has no barrier and favors the broken symmetry. For H–H distances of 3.4 au and less, $C_{2v}$ arrangements are lower in energy than their slightly distorted $C_s$ counterparts, thus indicating the existence of a barrier against going on to MgH + H. In between these two H–H distances, the increase in energy in distorting the $C_{2v}$ molecule is too slight to determine and hence the exact location of the lowest energy exit point from the $C_{2v}$ surface remains somewhat uncertain. However, an exit "seam" can be approximately given by $3.4 < R_{HH} < 3.8$ au and $R_{MgH} \approx 3.6$ au which is depicted by the solid-line seam in fig. 1. Along this seam, the barrier to reactions giving MgH + H is between 0.7 kcal and 1.8 kcal/mole above the reaction endothermicity. This seam represents our prediction of that portion of the $C_{2v}$ surface through which reactions to MgH + H can proceed with the least total energy.

It should be noted that because the minimum barrier for reaction occurs at fairly large H–H separations, $H_2$ vibrational energy may be especially effective in overcoming the endothermicity of this reaction. In fact, the nature of the $C_{2v}$ potential energy surface suggests that $H_2$ vibrational energy should be more effective than Mg–$H_2$ translational energy in causing reaction. If the SCF-level energy surface described above was quantitatively correct, reaction (1) would be made essentially thermoneutral by only one quantum of $H_2$ vibrational energy, whereas the isotopically substituted reaction $Mg + D_2 \rightarrow MgD + D$ would require higher $D_2$ vibrational excitation. Experimental evidence to date gives no indication of vibrational versus translational activation since the initial quantum states have been prepared only in Boltzmann equilibria [8,9].

The behavior of the potential energy surface for a linear "end-on" approach was also examined. To correlate with the reaction products of symmetry $^2\Sigma$ MgH and $^2S$ H, one must employ an SCF wavefunction having $^3\Sigma$ symmetry. The $4a_1^2 5a_1 2b_1\ ^3B_1$ and $4a_1^2 5a_1 2b_2\ ^3B_2$ states were not examined because they correlate with $^3\pi$ MgH and H atoms. Hence, we carried out our SCF calculations using the orbital occupancy $4a_1^2 5a_1 6a_1$ which corresponds to $\sigma_g^2$3s Mg 3p Mg for $H_2$ + Mg and $\sigma_{MgH}^2$, 1s H, sp Mg for H + MgH. Exploratory calculations with the minimal basis set indicated that the linear approach of Mg, with relaxation of the $H_2$ bond length, is highly repulsive, as was expected. These calculations also indicated that the barrier to removal of the outermost hydrogen along the relaxation path's entrance channel is very high ($\geqslant$14 kcal/mole) and is located at a point where the distance from the magnesium to the nearest hydrogen is nearly the equilibrium bond length of MgH (3.3 au). Forceful separation of the hydrogens revealed a barrier to hydrogen separation with a saddle point located at an Mg–H distance of $\approx$3.6 au and an H–H distance ($\approx$2.2 au) considerably greater than that of $H_2$ (1.4 au). Calculations with our larger basis fixed the location of the saddle point at Mg–H and H–H distances of 3.59 and 2.14 au, respectively. The height of this barrier at this saddle point was found to be 14.3 kcal/mole above the reaction endothermicity. This is much higher than the analogous SCF-level barrier for the $C_{2v}$ approach. One can thus conclude that $C_{2v}$ attack seems to be energetically favored over end-on attack. Because these results were obtained using SCF-level wavefunctions, they might not be accurate in an absolute sense but they are likely to yield reliable relative energetics for the $C_{2v}$ and linear approaches because for both geometries the single configuration wavefunctions properly connect the reactant and saddle point orbitals' symmetries.

The final question considered in this study was the nature of the reaction exit path. We have already indicated that the "seam" shown in fig. 1 describes the region of $C_{2v}$ space where, for the least energy, distortions away from $C_{2v}$ geometry begin to be energetically favorable. What we now wish to address is what geometrical changes characterize the minimum energy path leading to MgH + H. Exploratory calculations with the minimal basis indicate that at H–H separations of up to 4.0 au the minimum energy path in the distorted $C_s$ region favors bent arrangements with the near hydrogen in between the magnesium and the separating hydrogen. Since, for geometric reasons, insertion cannot take place at H–H separations less than $\approx$6.6 au (twice $R_e$ for MgH), tests were made to determine the potential surface's behavior at large H–H distances and to attempt to understand how the system might evolve from the seam in the $C_{2v}$ surface discussed above toward lower-energy $C_s$ geometries. First, the distances from the magnesium to the near hydrogen and the far hydrogen were fixed at 3.3 au ($R_e$ for MgH) and 7.3 au, respectively. The longer MgH distance was chosen based on the knowledge that for linear HH Mg an H–H distance of 4.0 au corresponds to an essentially broken $H_2$ bond. Then the system was varied from an end-on arrangement ($R_{HH}$ = 4.0 au) to an inserted arrangement ($R_{HH}$ = 10.6 au). Along this "path", a minimum energy was found at an H–Mg–H angle of 66° ($R_{HH}$ = 6.7 au). Given this result, the H–H distance was then frozen at 6.7 au and the shorter Mg–H distance at 3.3 au. The Mg atom was then rotated from the end-on arrangement (long $R_{Mg-H}$ = 10.0 au) to the inserted geometry (long $R_{Mg-H}$ = 3.4 au) along which only the angle and the longer Mg–H distance is changed. The energy minimum along this "path" was found to occur at the same point as before. Motion along the first "path" can be viewed as involving a MgH molecule and an H atom whose distance to the Mg is fixed (7.3 au) while the H–H distance is varied. The second "path" fixes the H–H distance and one of the Mg–H distances (at $R_e$ of MgH) while the second Mg–H distance is varied. Similar tests at longer distances were not tried, since the separations were approaching atomic scale "infinite distance", where energy is independent of orientation. It is noted in passing, however, that for H–H distances greater than 2.6 au, most local minima were found to have an H–Mg–H angle of $\approx$60°. These results indicate that once the reactants reach the "seam" region of fig. 1, the energetically most favorable distortions away from $C_{2v}$ geometry involve motion of one H atom away from the center of mass of the product MgH combined with rotation of the nascent MgH molecule.

## 5. Summary

In summary, the most significant information obtained in this theoretical study of reaction (1) concerns the probable nature of attack which can lead to MgH + H. It was found that the reaction can proceed from a side-on approach with a barrier of not more than 2 kcal/mole above the reaction endothermicity. In contrast, end-on attack exhibited a barrier above endothermicity that was ≈14 kcal/mole, thereby showing side-on attack to be highly favored. The shape of the potential energy surface for side-on attack indicates that vibrational excitation of $H_2$ should be more effective than relative translational energy in causing reaction. Furthermore, the nature of the occupied molecular orbitals indicates that partial charge transfer interactions do play some role in the reaction mechanism. Finally, no indication of a bound or metastable triplet state of $MgH_2$ was found.

## Acknowledgement

We gratefully acknowledge the advice and assistance of Drs. Ron Shepard and Ajit Banerjee during the course of this work. This research was supported by the National Science Foundation, Grant No. 7707603. Funds for the purchose of the DEC 20 Computer with which the calculations were performed were also provided in part by the National Science Foundation.

## References

[1] G. Cario and J. Franck, Z. Physik 11 (1922) 161.

[2] J. Calvert and J. Pitts, Photochemistry (Wiley, New York, 1966).

[3] D.L. King and D.W. Setser, Ann. Rev. Phys. Chem. 27 (1976) 407, and references therein.

[4] W.H. Breckenridge and A.M. Renlund, J. Phys. Chem. 82 (1978) 1484, and references therein.

[5] A.B. Callear and J.C. McGurk, J. Chem. Soc. Faraday Trans. II 68 (1972) 289.

[6] W.H. Breckenridge and A.M. Renlund, J. Phys. Chem. 83 (1979) 1145.

[7] S. Yamamoto, T. Takei, N. Nishimura and S. Hsegawa, Bull. Chem. Soc. Japan, 53 (1980) 860.

[8] R.P. Blickensderfer, W.H. Breckenridge and D.S. Moore, J. Chem. Phys. 63 (1975) 3681.

[9] W.H. Breckenridge and W.L. Nikolai, J. Chem. Phys. 73 (1980) 763.

[10] W.J. Balfour and B. Lindgren, Can. J. Phys. 56 (1978) 767.

[11] S. Lin and R.E. Weston Jr., J. Chem. Phys. 65 (1976) 1427, 1443.

[12] B. Earl and R. Herm, J. Chem. Phys. 60 (1974) 4568.

[13] D.A. McGillis and L. Krause, Can. J. Phys. 46 (1968) 1051.

[14] E.S. Hrycyshyu and L. Krause, Can. J. Phys. 48 (1970) 2761.

[15] J. Elward-Berry and M.J. Berry, J. Chem. Phys. 72 (1980) 4510, and references therein.

[16] P. McGuire and J.C. Bellum, J. Chem. Phys. 71 (1979) 1975.

[17] S. Huzinaga and C. Arnau, J. Chem. Phys. 53 (1970) 348.

[18] A. Veillard, Theoret. Chim. Acta 12 (1968) 405.

[19] T.H. Dunning Jr., J. Chem. Phys. 53 (1970) 2823.

[20] R. Ahlrichs, F. Keil, H. Lischka, W. Kutzelnigg and V. Staemmler, J. Chem. Phys. 63 (1975) 455.

[21] W. Meyer and P. Rosmus, J. Chem. Phys. 63 (1975) 2356.

[22] R.P. Saxon, K. Kirby and B. Liu, J. Chem. Phys. 69 (1978) 5301.